Title
MEASUREMENT OF THE HIGH ENERGY COMPONENT OF THE X-RAY SPECTRA IN THE VENUS ECR ION
SOURCE

Authors
Leitner, Daniela
Benitez, Janilee Y.
Lyneis, Claude M.
et al.

Publication Date
2008-06-04

Peer reviewed

Measurement of the high energy component of the x-ray spectra in the VENUS ECR ion source

D. Leitner[1*], J.Y. Benitez[1], C.M. Lyneis[1], D.S. Todd[1],

[1] Lawrence Berkeley National Laboratory, One Cyclotron Road, Berkeley, CA, 94720

T. Ropponen[2], J. Ropponen[2], H. Koivisto[2]

[2] Department of Physics, Accelerator Laboratory, University of Jyväskylä, FIN-40014, Finland

S. Gammino[3]

[3]INFN-Laboratori Nazionali del Sud, Catania, Italy

High performance electron cyclotron resonance (ECR) ion sources, such as VENUS (Versatile ECR for Nuclear Science), produce large amounts of x-rays. By studying their energy spectra, conclusions can be drawn about the electron heating process and the electron confinement. In addition, the bremsstrahlung from the plasma chamber is partly absorbed by the cold mass of the superconducting magnet adding an extra heat load to the cryostat. Germanium or NaI detectors are generally used for x-ray measurements. Due to the high x-ray flux from the source, the experimental set-up to measure bremsstrahlung spectra from ECR ion sources is somewhat different than for the traditional nuclear physics measurements these detectors are generally used for. In particular the collimation and background shielding can be problematic. In this paper we will discuss the experimental set-up for such a measurement, the energy calibration and background reduction, the correction for detector efficiency, the shielding of the detector and collimation of the x-ray flux. We will present x-ray energy spectra and cryostat heating

* Abstract, published as part of the Proceedings of the 12th International Conference on Ion Sources, Jeju, Korea, August 2007.

rates in dependence of various ion source parameters such as confinement fields, minimum B-field, rf power and heating frequency.

* corresponding author: dleitner@lbl.gov

1. Introduction

The VENUS ECR ion source at the Lawrence Berkeley National Laboratory (LBNL) has been designed for optimum operation using 28 GHz plasma heating frequency. The maximum axial magnetic confinement fields are 4 T at injection and 3T at extraction and are generated by three solenoid coils. A wide range of minimum B fields (Bmin) between the magnetic mirrors can be tuned by changing the current of the middle coil. The radial field at the plasma chamber wall can be operated at fields up to 2.1 Tesla (slightly more than twice the resonant field for 28 GHz ($B_{ECR\ 28\ GHz}$=1T)). VENUS has been operated routinely using 28 GHz as its main heating frequency since 2004 and has produced many world record beams [1,2]. Besides 28 GHz, 18 GHz can be injected as a second frequency for double frequency heating or used for single frequency heating at 18 GHz ($B_{ECR\ 18\ GHz}$=0.64T). The source design and its performance are described in detail in [1,2] and several references within these papers. Because VENUS is a fully superconducting ECR ion source, its magnetic confinement field can be tuned over a wide range. This flexibility makes VENUS a good tool to study frequency scaling laws and the influence of the magnetic field gradient at the resonance zone.

Bremsstrahlung spectroscopy is a standard plasma diagnostic tool and has been extensively used in fusion devices and ECR ion sources to diagnose the hot electron population [3-5]. Two processes in the plasma lead to the emission of bremsstrahlung. First bremsstrahlung is created by electron-ion collisions within the plasma volume. Secondly bremsstrahlung is emitted by electrons that are lost to the plasma chamber wall and lose their energy through interaction with the wall material. The x-rays produced by these processes can penetrate through the plasma chamber wall. They cause x-ray radiation in the vicinity of ECR ion sources and can add a substantial heat load to the cryostat (see section 7), when they are absorbed in the cold mass. To minimize and control this radiation, an understanding of the expected x-ray energy and flux is essential for the design and operation of superconducting sources. At the VENUS ECR ion source measurements of the bremsstrahlung spectra have been proven to be a particularly powerful tool for the characterization and understanding of the source and minimization of the x-ray heating load from the plasma. Previous measurements of the axial bremsstrahlung's spectra of the VENUS ECR ion source led to the design of a plasma chamber that incorporates a 2mm Ta shielding wall around the chamber[6]. This Ta shielding reduces the effective x-ray flux by a factor of 10 and has allowed the source to operate at higher rf power and a wider range of magnetic confinement fields. Similar designs now incorporated in other superconducting ECR ion source under construction [7,8]. However, as shown in reference [6] Ta becomes transparent for x-ray energies above 400keV, and it is these high energy x-rays that contribute most to the cryostat heating. These 'ultra hot' electrons continue to present a challenge for the design and operation of next generation superconducting ECR ion sources using microwave heating frequencies of 28 GHz and higher and must be studied carefully to further advance the field of high field superconducting ECR ion sources.

2. Experimental set-up

Due to the high x-ray flux and the high x-ray energies produced by the ECR ion source, the experimental set-up to measure bremsstrahlung spectra is somewhat different than for the traditional nuclear physics measurements these detectors are generally used for. In particular the collimation and background shielding have to be done carefully and are described in detail below. It is particular important to ensure that the shielding is adequate otherwise unphysical high energy "bumps" appear in the x-ray spectra in the energy range where 1 to 2 cm of lead shielding does not provide enough attenuation (Fig.2). These 'bumps' disappear as more lead shielding is added around the collimator. The experimental set-up used for all the measurements presented is shown in Fig.1. The x-ray signal was collimated by a 127 mm long heavy-metal collimator composed of 95% W and 5% Cu located 2.37m away from the extraction aperture. The collimator block has a 1mm square groove along the length, which is aligned with the extraction hole of the VENUS ECR ion source. In addition, the collimator is surrounded by lead shielding blocks to minimize x-ray coming from other areas of the plasma chamber or are scattered outside the collimator from reaching the detector. The NaI phototube detector is placed about 2.16m away to reduce the dead time of the detector. In addition, the detector is surrounded by 5cm thick lead shielding blocks to minimize background radiation (coming from other X-ray sources in the vicinity (e.g. the AECR ion source). Finally, another entrance collimator of 12.7mm diameter is placed before the detector. With the collimator and all the shielding in place the x-ray leakage to signal ratio is reduced to

1:250. The energy calibration of the spectrum is done using a ^{207}Bi source, using three characteristic gamma lines at 569, 1063keV and 1770 keV.

As the ECR ion sources are located directly above the cyclotron vault, the detector must be shielded from the cyclotron's magnetic stray field. Therefore, the detector was placed into a 6mm thick iron shield. In addition, phototube detectors can experience energy calibration drifts due to ambient temperature changes. The temperature drift of our detector was measured to be less than 2% for a temperature change of 10 degrees. Finally, the change of the energy calibration due to count rate changes was found to be less than 1%, when varying the count rates from 800 Hz to 30000Hz. However, over several days of operation, the energy calibration of the detector can drift a few percentages, which we were unable to eliminate. Therefore we recalibrate the detector for each measured spectrum to avoid any systematic errors. The spectra were not corrected for detector efficiency across the energy range. Since the detector efficiency is not flat across the energy range, but lower for higher energies. Therefore the spectral temperatures and absolute x-ray intensity will be underestimated for higher energies. The maximum acceptance angle of the collimator system is .2 degree. This acceptance angle translates to a 14mm diameter circle at the extraction plate. Since the extraction aperture of the VENUS ECR ion source has a diameter of 8mm, bremsstrahlung created by electrons lost to the extraction aperture wall can be detected in our set-up. When the collimator geometry and the angular distribution of the bremsstrahlung were simulated with GEANT4[9], it was found that changes of the shape of the energy spectrum due to scattering effects of x-rays in the collimator can be neglected and that the produced bremsstrahlung is mainly forward directed. This also suggests that a substantial part of the x-rays detected with the current experimental set-up is coming from electrons lost on the extraction plate.

3. Experimental Results with VENUS

For this paper we focus on a comparison of the x-ray spectra using two axial magnetic field configurations. Both are typical field configurations which are used to achieve high intensity, high charge state ion beams. In the first configuration we are using a minimum B field of .44T, in the second configuration we are using a minimum B field of .67T to .7T. The sextupole field and the peak mirror fields were held nearly the same during all experiments. All other source parameters such as gas flow and gas mixing ratio were kept constant. However, the biased disk was adjusted for each configuration to optimize the stability of the ECR ion source. Figure 3 shows the magnetic field configurations used for all the measurements presented in this paper. However, changing the minimum B field of the source changes the resonance zone volume. The resonance zone volume is about 40% smaller when the minimum B field is raised from .44T to .67T.

The following sections summarize the results of three experimental series. In section 4, the influence of RF power on the electron energy distributions and on the total x-ray flux is presented. In section 5, the x-ray spectra obtained using 28 GHz plasma heating are compared to spectra using 18 GHz microwave heating. In sections 6 and 7, the source performance and the x-ray heat load into the cryostat are compared for single frequency operation at 28 GHz using a minimum B field of .67T to double frequency operation using 18 and 28 GHz heating and a minimum B field of .44T.

4. Influence of the microwave power on the energy distribution of the x-ray spectra

X-ray spectra were measured for microwave power levels from 500W up to 7000W using single frequency heating at 28 GHz. The amount of x-rays produced increase nearly linearly with power in both cases, but as it can be seen from Fig. 4a and Fig. 4b increasing the microwave power for a given axial field configuration does not change the slope of the semi-logarithmic plot. . However, the x-ray spectra extend up to much higher energies for Bmin of .7T compared to Bmin of .44T. To compare x-ray spectra measured with different magnetic field configurations, the spectral temperatures defined in [4,6] have been determined (Fig. 5a and Fig.5b). For this purpose a linear fit to the semi logarithmic plot was determined and the reciprocal of the line's slope yields as a spectral temperature (T_s) in keV. This spectral temperature is a relative indication of the temperature of the hot electrons, not a direct measure of the temperature distribution of the hot electrons in the plasma.

As shown in the figure 5, the spectral temperatures are nearly independent of the microwave power injected. This suggests that increasing the rf power mainly increases the plasma density, but does not (or very little) affect the energy distribution function. However, two or more slopes (temperatures) are needed to fit the semi logarithm plot for higher minimum B fields, while the spectra obtained with a lower minimum B field can be fit by one slope.

The higher spectral temperatures measured for high minimum B fields could suggest that the heating efficiency is higher for lower magnetic field gradients at the resonance zone. This finding is consistent with the simple heating models suggested by Jongen in 1982[10] and Koivisto in 1999 [11], that predicts a more efficient acceleration process of the electrons when the resonance zone is crossed at a lower field gradient. This is also consistent with previously published results which found that higher ion beam intensities can be extracted for higher minimum B fields [2,7].

5. Comparison of 28 GHz heating with 18 GHz heating at scaled fields at Bmin/Becr of .70 and .47

To test ECR scaling laws [12], the bremsstrahlung spectra using single frequency heating at 28 GHz were compared to spectra obtained with 18 GHz. To ensure that the magnetic confinement, the magnetic field gradient, and the size of the resonance zone are identical, the magnetic fields (including the sextupole fields) were carefully scaled according to the ratio of 18/28. All other source parameters were kept constant.

For single frequency heating at 18 GHz a similar trend in the x-ray spectra between the steep (low minimum B field) and shallow (high minimum B field) magnetic field gradient is observed. The spectrum extends to higher energies and has a higher spectral temperature for the higher Bmin (compare Fig.6, blue curves). In addition the slopes of the spectra do not change with increasing power. However, when the 18 GHz spectra are compared to 28 GHz spectra using the same injected power and scaled magnetic fields, the latter spectra extend up to much higher energies and have higher spectral temperatures. This suggests that 28 GHz heating (or higher frequency heating in general) is more efficient than lower frequency heating. This result is consistent with a model developed by Girad et al. [13], which predicts higher mean electron energies for increased heating frequencies.

The development of a high energy tail in the electron energy distribution for the 28 GHz heated plasma can explain why the heated x-ray heat load from a 28 GHz heated plasma is much higher than what could be expected from the simple increase in electron density using the frequency scaling law[14]. Since the Ta shield and the plasma chamber walls become almost transparent for x-rays above 300keV, the high energy x-rays are primarily responsible for heating the cryostat (see section 7).

6. Comparison of the Ion Source Performance and X-ray spectra for an axial magnetic field profile with a Bmin of .67T and .45T

The goal of these measurements was to systematically compare the high charge state performance using a middle field of .45T and double frequency heating to single frequency heating using a middle field of .67T. For the measurements presented in this paper, the source was operated with xenon using oxygen as mixing gas, but similar trends have been found for other ion beams such as argon, krypton or uranium etc..

As shown by many authors before, for the single frequency heated plasma, the high charge state performance of the ECR ion source is strongly dependent on the minimum B field [7,14,15]. For VENUS an optimum can be found for a minimum B field of .64 to .75 Tesla[14], which results into a magnetic field gradient at the resonant zone of about 0.08 to 0.07 T/cm. Good plasma stability can be achieved above microwave powers above 2kW or a power density of 220W/liter. When the gas flow into the source is unchanged, the charge state distribution slowly shifts to higher charges states as more power is injected. For example, the peak of the xenon charge state distribution shifts from 30+ to 32+ using

4, 5 and 6 kW of 28 GHz microwave power. In Fig. 7 shows the increase in high charge state current for Xe^{33+} to Xe^{39+} for this power range.

For the double frequency heated plasma, the large frequency gap between 18 and 28 GHz requires a relatively low minimum B field to enable the coupling of 18 GHz into the plasma. A typical magnetic field profile used for double frequency operation is shown in Fig.3 (dashed line). For 28 GHz heating, this field profile results in a relatively steep magnetic field gradient on axis at the resonant zone (.13T/cm) with a B_{ECR}/Bmin ratio of .45. For 18 GHz heating, this profile results in a gentle magnetic field gradient (0.075T/cm) with a B_{ECR}/Bmin ratio of .70 T. The combination of these two frequencies in this mode enables a very stable operation of the VENUS ECR ion source and is the preferred mode to use when the source is conditioned after maintenance. The optimum ratio of 28 to 18 GHz microwave power was found to be about 85% of 28 GHz to 15% of 18 GHz. If a higher percentage of 18 GHz power is coupled into the plasma, no performance improvements are observed, but the source plasma becomes slightly unstable.

Both modes of operation (single and double frequency) produce high intensity, high charge state ion beams. In fact an identical high charge state performance can be achieved, but more microwave power is required for the double frequency mode. For example the same currents for Xe^{33+} to Xe^{39+} can be produced by using either 6 kW of 28 GHz microwave power in single frequency mode (with B_{ECR}/Bmin =0.67) or 7.5kW of 28 GHz and 1.3kW of 18 GHz power in double frequency mode. As an illustration, Fig. 8 shows the dependence of Xe^{35+} with power for those two modes. As can be seen from the graphs the source performance can be matched in each case, but more total power has to be used in the double frequency mode. If the x-ray energy spectra are compared for two tunes with identical high charge state, heavy ion currents, it is found that the numbers of counts in the low energy region of the spectra are very similar (Fig. 9). As expected (see section 4), the x-ray spectrum extends up to much higher energies for the higher middle field. However, since lower energy electrons have the highest ionization cross section, the result suggests that similar performance can be achieved if the warm electron density is matched in the two cases.

It is evident that in terms of power efficiency the gentle gradient is superior over the steep gradient double frequency mode. But from an operational point of view the double frequency mode with its steep gradient has clear advantages over the single frequency mode. Since the bremsstrahlung spectra for the steep gradient contain much fewer the x-rays in the energy region above 400keV (where the Ta shield around the plasma chamber is not effective), the resulting heat load into the cryostat is much smaller (see section 7)

If the charge state distributions of the ion beams extracted for each mode are plotted on top of each other, the xenon spectra are remarkably similar (Fig. 10). However, the oxygen mixing gas spectra is very different for the two modes. In the double frequency mode, the oxygen spectra is clearly peaked on high charge states, while in the single frequency mode the oxygen charges state distribution is much flatter. For example in the case of oxygen 7+ only 40euA are produced in the single frequency mode when the source is optimized for high charge state xenon ions, but 270 euA are produced in the double frequency mode. This shift in the mixing gas distribution is also reflected in an increase of total current when the source is switched from single to the double frequency mode as the oxygen ions are shifted towards higher charge states. In the moment we do not have an explanation for this phenomenon, but it has been experimentally observed for all heavy ions produced so far (Ar, Kr, Xe and U).

7. Heat load into the cryostat from bremsstrahlung

The emitted bremsstrahlung, created by electron-ion collisions within the plasma volume and by electrons lost to the plasma chamber wall, adds a substantial heat load to the ion source cryostat. To better understand the amount of power absorbed in the cold mass under various tuning condition, the heat load caused by x-ray absorption was measured in the VENUS source in dependence of coupled microwave power for the double and single frequency heated source. The heat load was determined by comparing the temperature rise of the liquid helium, when the helium reservoir was heated by a calibrated heater without plasma to the temperature rise observed when the source was operated at various microwave power levels. In Figure 11 the heat load into the cryostat is plotted for a Bmin of 0.45 T and Bmin of .64T. For a Bmin of .64T a heat load of about 1W/kW was found, while for the double frequency heated source, the heat load was determined to be only .1W/kW. The error bar indicates the range of heat load depending on the discharge pressure and the accuracy of the measurement. This big difference is caused by the high energy tail of the x-rays present in the spectra for Bmin fields of .6T and higher. Since the 2mm Ta shield becomes transparent for x-ray energies above 400keV, the shield looses its effectiveness at these energies and the bulk of these x-rays produced are absorbed in the cold mass.

8. Conclusion

A few conclusions can be drawn from the above measurements. A gentler magnetic field gradient at the resonant zone will result in a more efficient heating process and will lead to the generation of a hot electron tail in the electron energy distribution. This high energy tail is strongly affected by the ratio of Bmin/Becr and by the heating frequency. As expected, an ECR plasma heated with 28 GHz microwaves produces more x-rays than a plasma heated with 18 GHz microwaves if scaled fields are used and the mean electron temperature increases with frequency.

The high energy x-ray produced by 28 GHz heating using gentle magnetic field gradients at the resonant zone can not be effectively shielded by a few mm of Ta or other heavy metal x-ray shields. Therefore, they can penetrate into the cryostat, where they are absorbed by the cold mass and add a substantial heat leak to the cryostat system. As the comparison for 18 and 28 GHz spectra using scaled magnetic fields show, this problem can be expected to be worse for 4^{th} generation sources using microwave frequencies greater than 28 GHz. On the other hand generation of this high energy tail can be avoided using double frequency heated plasma and a combination of steep gradients for the main heating frequency (e.g. 28 GHz) and gentle gradients for the second frequency (e.g. 18 GHz). Using higher total power the performance of the source for gentler heating gradients can be matched, but with a much reduced heat load into the cryostat.

9. Acknowledgement

This work was supported by the Director, Office of Energy Research, Office of High Energy and Nuclear Physics, Nuclear Physics Division of the U.S. Department of Energy under Contract DE AC03-76SF00098.

10. References

1 D. Leitner, D.S. Todd, M.L. Galloway, and C.M. Lyneis, Journal of HEP&NP, Chinese Physical Society **31**, 1-7, http://www.impcas.ac.cn/usr/ecr/web/index.files/proceedings/D.Leitner.pdf, (2006).

2 D. Leitner, C. M. Lyneis, T. Loew, O. Tarvainen, D. S. Todd et al., RSI **77** (03A302), 03A303-301, (2006).

3 C. Barue, M. Lamoureux, P. Briand, A. Girard, and G. Melin, J. Appl. Phys. **76** (5), 2664 - 2669, (1994).

4 A. Girard, Rev. Sci. Instrum. 63 (4), April 1992 **63** (4), 2676-2682, (1992).

5 K. Bernhardi and K. Wiesemann, Plasma Physics **24** (8), 867 - 884, (1982).

6 C. M. Lyneis, D. Leitner, O. Tarvainen, D. Todd, S. Virostek et al., RSI **77** (03A342), (2006).

7 T. Nakagawa, Y. Higurashi, M. Kidera, T. Aihara, M. Kase et al., Rev. Sci. Instrum. **77**, 03A304, (2006).

8 G. Ciavola, S. Gammino, L. Celona, L. Torrisi, S. Passarello et al., RSI **77**, (2006).

9 S. Agostinelli, J. Allison, K. Amako, J. Apostolakis, H. Araujo et al., Nuclear Instruments and Methods A **506** (3), 250-303, (2003).

10 H. Koivisto, Rev. Sci. Instrument. **70** (7), 2979, (1999).

11 Y. Jongen, C. Pirate, and G. Ryckewaert, Centre dÉtudes Nucléaires-Grenoble Press, 3.1, (1982).

12 R. Geller, *Electron Cyclotron Resonance Ion Source and ECR Plasmas*. (Bristol, Institut for Physics Publishing, 1996).

13 A. Girard, C. Pernot, G. Melin, and C. Le´cot, Physical Review E **62** (1), 1182-1189, (2000).

14 D. Leitner and C.M. Lyneis, Proceedings of the Particle Accelerator Conference PAC'05, Knoxville, Tennessee, American Physics Society, IEEE, 2005

15 D. Hitz, A. Girard, G. Melin, S. Gammino, G. Ciavola et al., Rev. Sci. Instrum **73** (2), 509-512, (2002).

11. Figure Captures

Fig.1 Schematic of the experimental x-ray detector set up at the VENUS ECR ion source.

Fig. 2 If the shielding around the collimator is insufficient and unphysical high energy 'bump' appears in the x-ray spectra for the high energy region where the shielding becomes transparent. If more shielding is added this bump disappears (see Fig.4).

Fig.3 Axial Field Profile used for the single frequency heating at 28 GHz and double frequency heating at 18 and 28 GHz experiments. Only the middle field was changed while all other source parameter remained unchanged.

Fig.4 The bremsstrahlung spectra measured for a Bmin of .7 T (4a) compared to a Bmin of .45 T (4b).

Fig.5 The spectral temperatures (Slope of the x-ray spectrum) remain nearly constant with increasing power, but are a strong function of the magnetic field gradient at the resonant zone. Shown are the spectral temperatures obtained by fitting the spectra for a Bmin=.7T (5a) and Bmin=0.45T (5b)

Fig.6 Comparison of the bremsstrahlung spectra for 28 GHz heating to 18 GHz heating at scaled fields with a Bmin/Becr of .70 (7a) and .47 (7b)

Fig. 7 Xenon high charge state distributions for a single frequency heated plasma using a Bmin of .67 T (Bmin/Becr=.67) for 4, 5 and 6 kW of 28 GHz microwave power.

Fig.8 Comparison of the power dependence of Xe^{35+} production for a Bmin of .67T (singe frequency heating, 28 GHz) to a Bmin of .45T (double frequency heating 28+18 GHz)

Fig.9 The axial x-ray spectra for a Bmin of .44T (8.8kW power) in comparison to a Bmin field of .67T (6kW power). The Xe charge state distributions are nearly identical (Fig.11).

Fig.10 Charge state distribution (Xe + Oxygen) for the double frequency source and the single frequency heated source. The oxygen mixing gas charge state distribution is much more peaked towards the higher charge states for a Bmin of .45T, which increases the total extracted current from the ECR source

Fig. 11 Heat load into the cryostat at minimum B field of .64T and .45T in dependence of the injected microwave power. The error bar indicates the range of

heat load depending on the discharge pressure and the accuracy of the measurement.

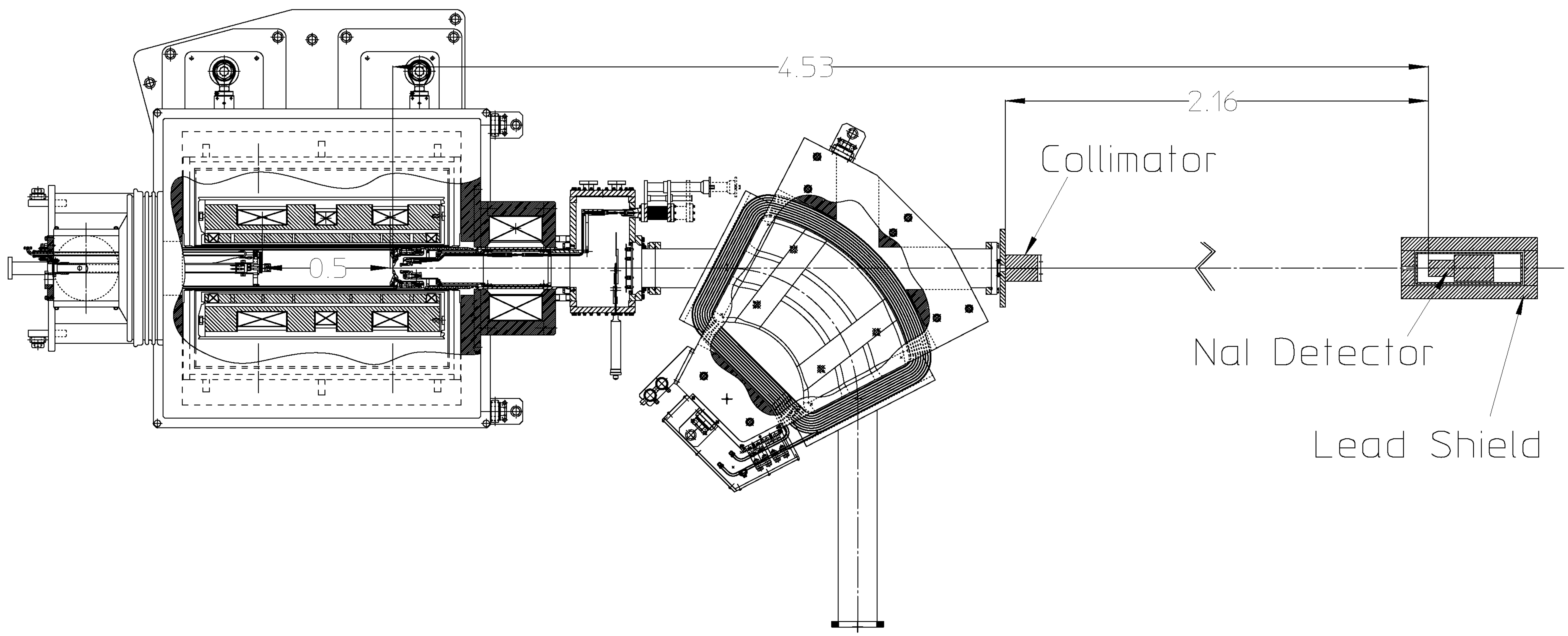

4.53
2.16
Collimator
0.5
NaI Detector
Lead Shield

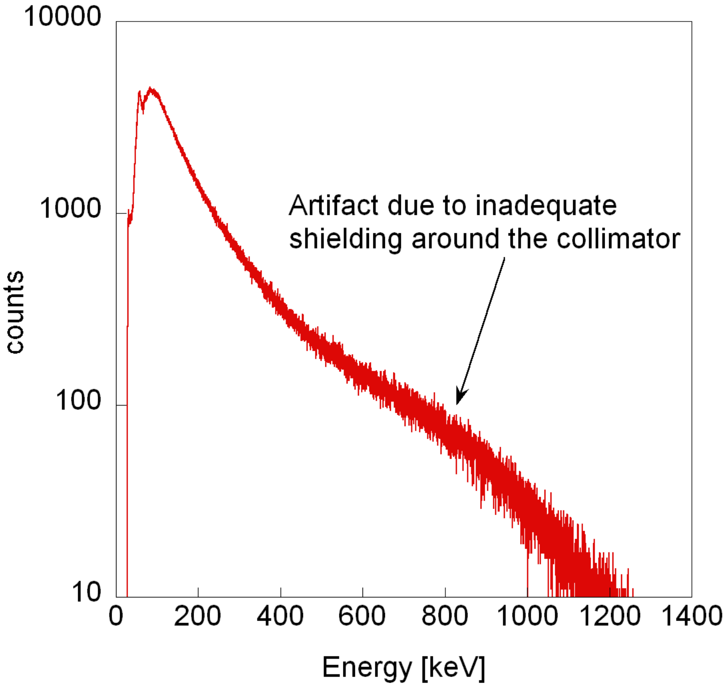
10000
1000
100
10
counts
0
200
400
600
800
1000
1200
1400
Energy [keV]
Artifact due to inadequate
shielding around the collimator

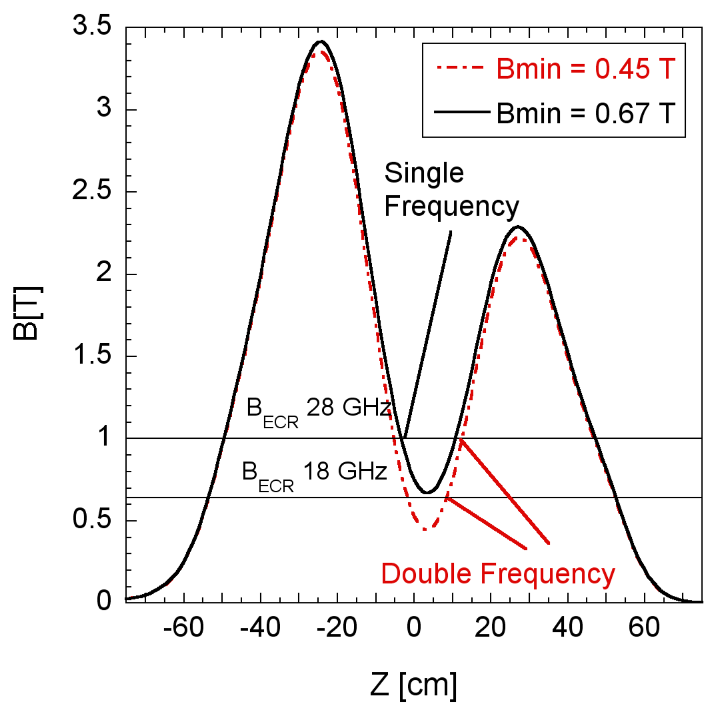

Bmin = 0.45 T
Bmin = 0.67 T
Single Frequency
B_ECR 28 GHz
B_ECR 18 GHz
Double Frequency
B[T]
Z [cm]
3.5
3
2.5
2
1.5
1
0.5
0
-60
-40
-20
0
20
40
60

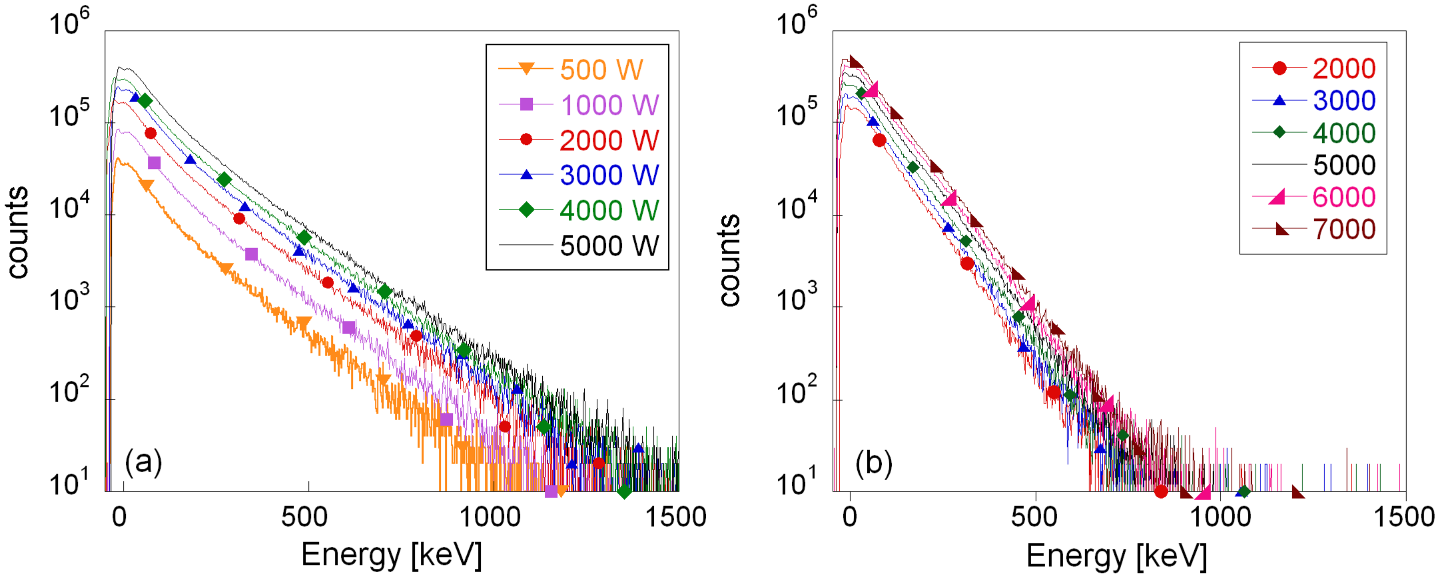

500 W
1000 W
2000 W
3000 W
4000 W
5000 W
(a)
counts
Energy [keV]
2000
3000
4000
5000
6000
7000
(b)
counts
Energy [keV]

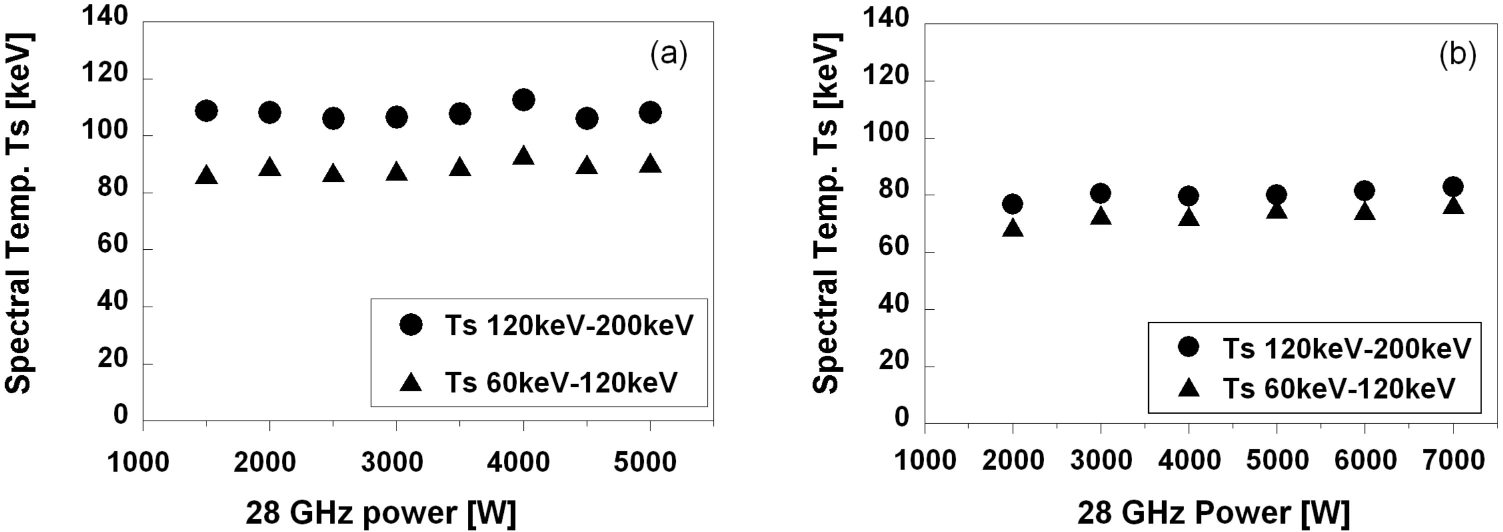
(a)
Spectral Temp. Ts [keV]
140
120
100
80
60
40
20
0
1000
2000
3000
4000
5000
28 GHz power [W]
Ts 120keV-200keV
Ts 60keV-120keV
(b)
Spectral Temp. Ts [keV]
140
120
100
80
60
40
20
0
1000
2000
3000
4000
5000
6000
7000
28 GHz Power [W]
Ts 120keV-200keV
Ts 60keV-120keV

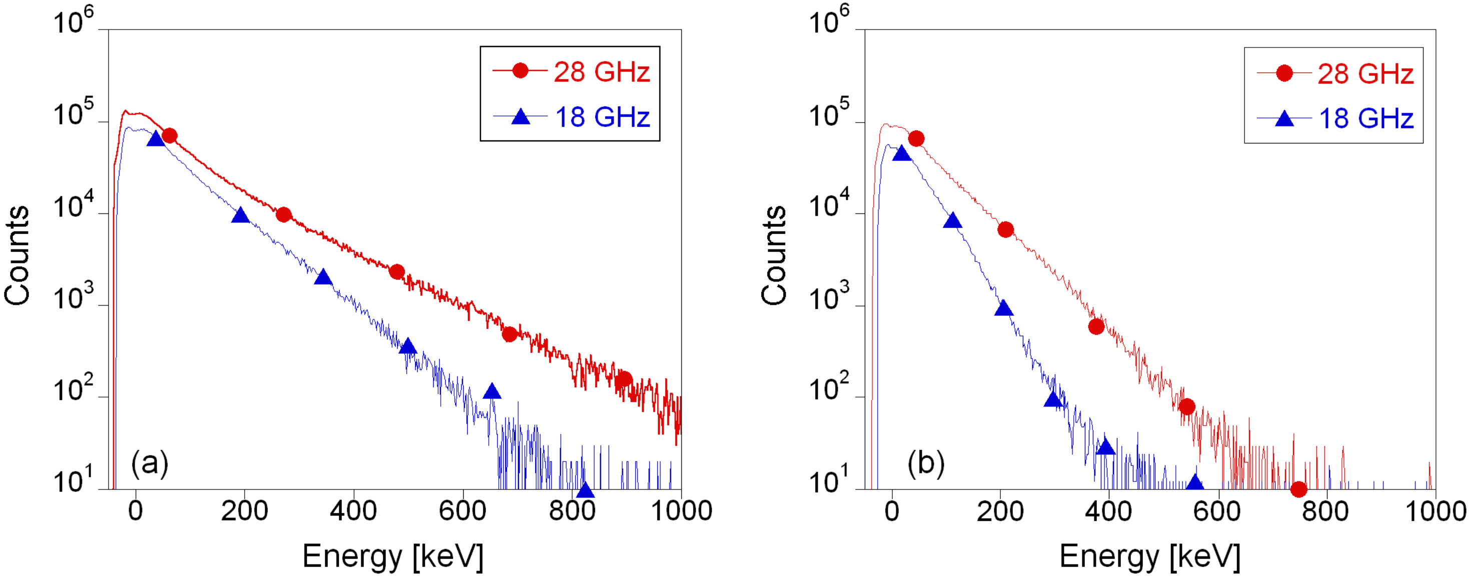

Counts
Energy [keV]
28 GHz
18 GHz
(a)
(b)
10^6
10^5
10^4
10^3
10^2
10^1
0
200
400
600
800
1000

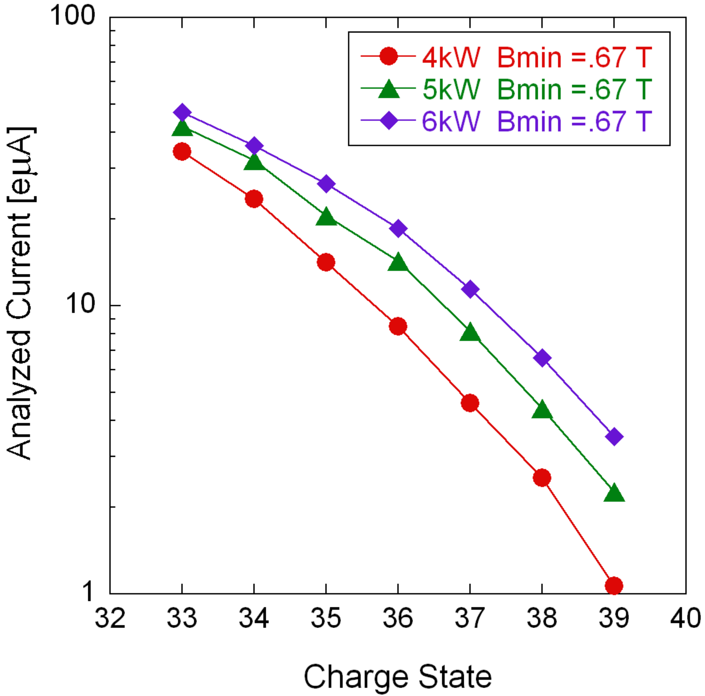

4kW Bmin =.67 T
5kW Bmin =.67 T
6kW Bmin =.67 T
100
10
1
32
33
34
35
36
37
38
39
40
Analyzed Current [eμA]
Charge State

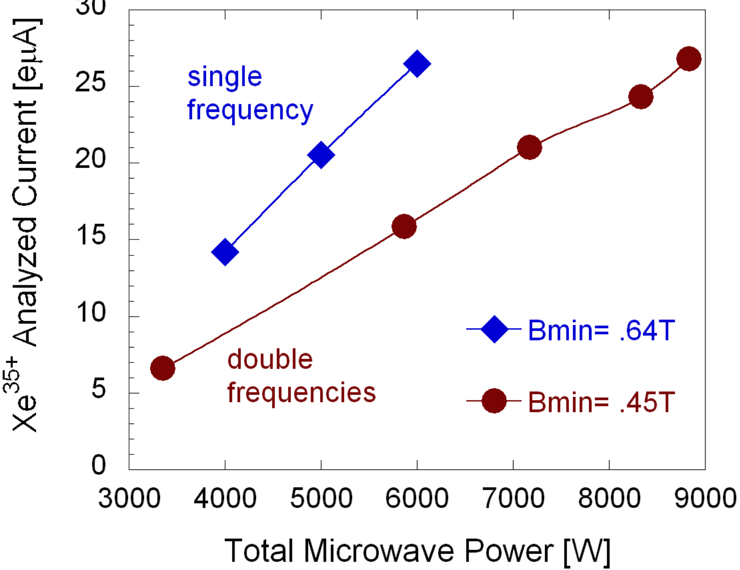

Xe^{35+} Analyzed Current [eμA]
Total Microwave Power [W]
single
frequency
double
frequencies
Bmin= .64T
Bmin= .45T
0
5
10
15
20
25
30
3000
4000
5000
6000
7000
8000
9000

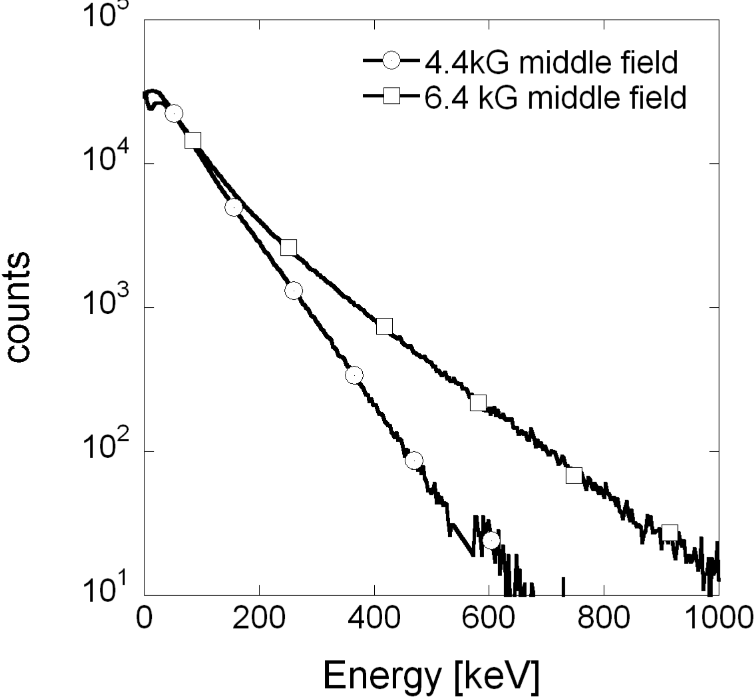
4.4kG middle field
6.4 kG middle field
counts
Energy [keV]
10^5
10^4
10^3
10^2
10^1
0
200
400
600
800
1000

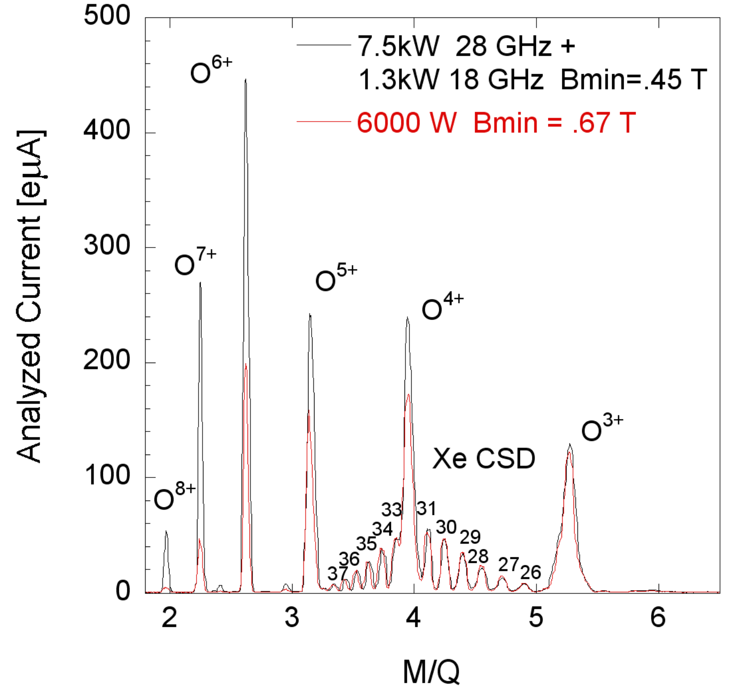

7.5kW 28 GHz +
1.3kW 18 GHz Bmin=.45 T
6000 W Bmin = .67 T
O6+
O7+
O8+
O5+
O4+
O3+
Xe CSD
37
36
35
34
33
31
30
29
28
27
26
Analyzed Current [eμA]
M/Q
500
400
300
200
100
0
2
3
4
5
6

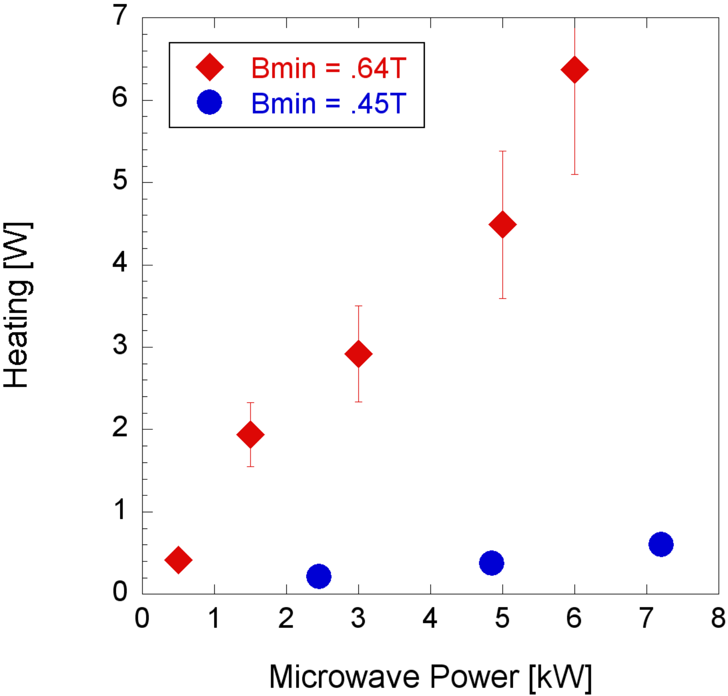

Bmin = .64T
Bmin = .45T
Heating [W]
Microwave Power [kW]
0
1
2
3
4
5
6
7
8